Unsteady Computational Fluid Dynamics of the axial flow generated by the rotation of an arm in swimming

Mathias Samson, Tony Monnet, Patrick Lacouture, Laurent David

Unsteady Computational Fluid Dynamics of the axial flow generated by the rotation of an arm in swimming

Mathias Samson, P' Institute, CNRS, University of Poitiers, ISAE ENSMA, RoBioSS team, Poitiers, France
Tony Monnet, P' Institute, CNRS, University of Poitiers, ISAE ENSMA, RoBioSS team, Poitiers, France
Patrick Lacouture, P' Institute, CNRS, University of Poitiers, ISAE ENSMA, RoBioSS team, Poitiers, France
Laurent David, P' Institute, CNRS, University of Poitiers, ISAE ENSMA, HydEE team, Poitiers, France

Abstract— In swimming, it has been shown experimentally that the arm rotation induce significant axial flow along the arm toward the hand, which acts favorably on propulsion (Toussaint et al., 2002). The purpose of this paper is then to numerical study the role of the axial flow on the propulsion of the hand and the forearm from a simple rotational movement. This study is based on unsteady RANS methodology (Samson et al., 2017). A comparison was made between two simulations in translation and rotation conditions. Velocities and depths of the hand were chosen so as to approach the actual conditions of swimming: the hand velocity is equal to 2.5 m $\cdot$ s^{-1}, and rotational velocity is equal to 5 rad $\cdot$ s^{-1}. Pressure, force and the spatio-temporal evolution of the vortices were used to the analysis. The results of the velocity fields of the flow show the presence of the axial flow along the hand and forearm in rotational configuration, but not in translation. The dynamic pressure gradients between the dorsal side of the hand and the elbow are higher in the rotational configuration (close to 2500 Pa) than in translation (close to 0 Pa). The hydrodynamic forces applied to the hand are greater in rotation than in translation (43 N vs 37 N respectively). At the beginning of the movement, two vortices are present all along the suction surface of the forearm and hand (a leading edge vortex on the little finger side and a trailing edge vortex on the thumb side). Next, these structures detach and are shedded into the wake. In both configurations, due to an accumulation of vorticity, a complex entanglement of vortex structures appears on the dorsal side of the hand. In the rotating configuration, there is more vortices on the dorsal side of the hand relative to the translation configuration. This can be explained by both the effect of the axial flow which translates the vorticity towards the fingertip, and at the same time the effect of the tip vortex at the fingertip which prevents the release of this vorticity (Von Ellenrieder et al., 2003).

Key words: axial flow, URANS methodology, CFD, pressure, vortices

1. Introduction

The propulsion in swimming is carried out essentially by the hands and the forearms (Maglischo, 2003; Takagi and Sanders, 2002). The cyclic action of these segments generates an unsteady flow which, by the principle of reciprocal actions (Newton's 3rd law) acts on the body surfaces. These actions are done through inertial effects (which act on the pressure component perpendicularly to the wall) and viscous effects (which act on the friction component tangentially to the wall).

Currently, the study of flow is carried out increasingly from an unsteady approach (Takagi et al., 2016). The studies are mainly made from experimental or numerical methods. The main tools of analysis are the pressure sensors (Kudo et al., 2010; Tsunokawa et al., 2018), either through Particle Image Velocimetry method (PIV, Takagi et al., 2014; Samson et al., 2015a) or by Computational fluid dynamics (CFD, Bixler and Riewald 2002; Samson et 2017). The present study is in a numerical approach to the flow. These different studies have shown a number of unsteady effects, including axial flow (Toussaint et al., 2002). This flow is generated by the incident velocity gradient along the arm (velocity differences between the shoulder (axis of rotation) and the hand (end of the segment)). These authors had experimentally shown that this axial flow acts favourably on propulsion by creating a pressure gradient between the elbow and the top of the hand.

However, this unsteady effect has been few studied in swimming (only one study to our knowledge, Toussaint et al., 2002). But this three-dimensional effect is very studied in the aquatic or aerial animal context (Ellington et al., 1996, Jardin and David, 2014, 2015), because its role is essential in the locomotion.

Thus, in order to discuss the role of the axial flow generated by the rotation of the arm in swimming, a numerical simulation has been carried out. This CFD study will compare the flow generated along the hand and the forearm in two configurations: one in transla-

tion and one in rotation. The goal is to better understand the role of axial flow along the hand and forearm in the propulsive mechanisms in swimming, notably from the analysis of the vortices structures.

2. Method

2.1 Numerical model

The numerical simulation was carried out using the URANS (Unsteady Reynolds Averaged Navier-Stokes) methodology, with moving mesh method in free surface condition (Samson et al., 2017). The governing equations are three-dimensional incompressible Navier-Stokes equations, and spatial discretization is based on a finite-volume method on unstructured meshes. The unsteady RANS equations were closed by a turbulence model (k-ω SST) and numerical simulations have been carried out with the STAR-CCM+® software.

An overset mesh method is employed in order to simulate the movements of the hand-forearm segment. The computational mesh created for the "overset region" (sphere of 1m in diameter containing 820,000 cells) around the hand-forearm moves in the fixed "background mesh" (parallelepiped 5m x 3m x 1m, containing 280,000 cells) in accordance with a stroke path. Two *inlet* boundaries were defined. A first, vertical, composed of an air/water in variable composition (managed by a field function), the input velocity is equal to 0 m · s^{-1} for reproducing the condition of a fluid at rest. The second (top surface) consists only of air. An *outlet* boundary (in pressure condition) is composed of an air/water varying in composition to ensure the conservation equations. Both sides of the volume are defined as a *symmetry plane*. The hand and forearm segment (of an expert swimmer) were scanned and digitized by a Minolta VI-900 scanner and imported in STL-file format (STereoLithography). The length of the hand is equal to 0.20 m, the width is equal to 0.10 m, and the length of the forearm is equal to 0.32 m. The projected area of hand and forearm are respectively 0.018 m^2 and 0.037 m^2.

The velocity of the hand-forearm segment is expressed in a fixed pool-centric reference system (Fig.1): (X_0, Y_0, Z_0) where X_0-axis is the backward direction, Z_0-axis is the vertical upward direction and Y_0-axis is perpendicular to X_0. A local reference system has been defined: (X, Y, Z) linked to the hand. X is the axis which passed through finger tip (FT) and W (wrist) which is the middle of [RS, US] segment (RS: radial styloid, US: ulnar styloid). Z was perpendicular to the (X, RS-US) plane and Y was perpendicular to X and Z (Monnet et al., 2014).

2.2 Kinematics of the hand-forearm stroke movement

Two simulations were carried out: one in translation and one in rotation (Fig. 1). For both simulations, the movement involves moving from rest to a constant velocity during 0.8 second: $V_{segment}$ = 2.5 m · s^{-1} for the translation and Ω_y= 5 rad · s^{-1} for the rotation (in order to obtain in rotation a velocity of the hand close to that obtained in translation). Velocities and depths of the hand were chosen so as to approach the actual conditions of swimming (elbows depth is 0.2 m). Angle of attack is close to 60° (with the little finger as the leading edge), which is the average measured during the insweep phase (Samson et al., 2015b). Angle of attack is defined as the angle between the velocity vector of the hand and its projection onto the plane of the hand (X, Y).

2.3 Calculation of dynamic pressure and force of the hand

2.3.1 Dynamic pressure

We chose to calculate the dynamic pressure because the rotational configuration induces variations of hydrostatic pressure over time for a same point of the segment, which is not the case in translation. This will allow to analyse only the hydrodynamic effects due to flow. Dynamic pressure (P_d) is calculated by subtracting the hydrostatic pressure to the total pressure in order to overcome the effect of the water depth.

$$P_d = \frac{1}{2}\rho V^2 \quad (1)$$

With ρ is the density of the fluid and V is the local flow velocity,

2.3.2 Hydrodynamic forces

Hydrodynamic forces depend directly on the flow of water on the swimmer. They represent the action, over the entire body surface, of the inertial and viscous effects of the flowing fluid. Inertial effects act on the pressure component (perpendicular to the wall) and the viscous effects on the friction component (tangential to the wall). The hydrodynamic force (F_h) is the integral of these components over the entire studied surface:

$$\vec{F_h} = \underbrace{\iint_S -P_d\vec{n}\,dS}_{\text{Pressure component}} + \underbrace{\iint_S \bar{\bar{\tau}}\vec{n}\,dS}_{\text{Friction component}} \quad (2)$$

τ is the tensor of viscous stresses and accounts for the viscous effects of fluid on body segments. τ is equal

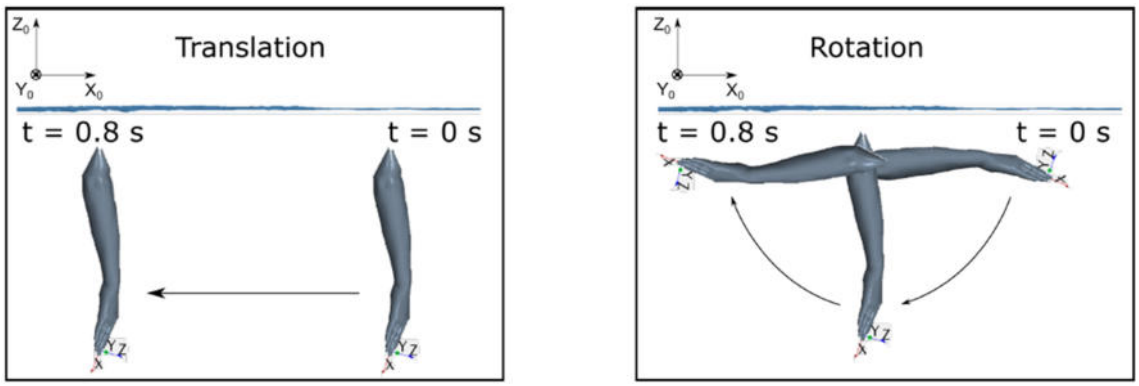

Fig. 1 Representation of the movement of hand-forearm segment in both configurations: in translation (at left) and in rotation (at right).

to:

$$\mu\left(\frac{\partial V_i}{\partial x_j} + \frac{\partial V_j}{\partial x_i}\right) \quad (3)$$

With μ the dynamic viscosity. P_d is the dynamic pressure (Eq. 1) and n is the normal vector for each surface element dS. The norm of the hydrodynamic force will be calculated in order to compare the effects of the flow in the segment in translation and rotation configurations.

2.4 Flow visualisation and vortex structure identification

Propulsive mechanisms are related with unsteady behavior of vortices (Matsuuchi, 2009). Q criterion and vorticity were chosen to study the spatio-temporal evolution of the vortex structures (Samson et al., 2017). Vorticity is defined as the rotational of the velocity, which expresses the trend of the field lines of a vector field to rotate around a point. Moreover, a positive Q criterion value characterises a vortex structure. Vorticity is used in complement of Q criterion in order to qualify the vortex intensity.

3. Results

3.1 Velocity fields

Figure 2 shows that the axial flow is present in the rotational configuration (Fig. 2b), unlike that in translation (Fig. 2a).

3.2 Dynamic pressure and hydrodynamic force acting on the hand

In Figure 3a, we see that the dynamic pressures calculated of a point on the palm of hand (grey and black dotted lines respectively in rotation and in translation) are very close (about 2500 Pa). This confirms the good proximity between the local velocity with respect to the hand: the flow of water that arrives on the hand is at a close velocity, the dynamic pressure is therefore close (Eq. (1)).

Figure 3a shows that the dynamic pressure gradients between the dorsal side of the back of the hand and the elbow are higher in the rotational configuration (close to 2500 Pa, the grey solid line) than in translation (close to 0 Pa, the black solid line). Moreover, the average hydrodynamic forces applied to the hand are greater than in translation (about 15%, 43 N vs 37 N respectively, Figure 3b).

4. Discussion

It appears that the rotation of the arm induces an axial flow which generates a pressure gradient from the elbow to the back of the hand. This result is in agreement with that of obtained by Toussaint et al., in 2002., and referred to as “pumped-up propulsion” term. In order to better understand this occurred, a study of the spatial and temporal evolution of vortex structures is carried out (Figure 4). The twelve left-hand figures show the vortices structures in translation, in front and lateral sides, at different times. The twelve right-hand figures show the evolution of vortex over time in the rotating configuration for the two same point of views.

At t = 0.05 s, two counter-rotating vortices are present all along the back of the forearm and hand (TEV_1^{trans}, LEV_1^{trans} and TEV_1^{rot}, LEV_1^{rot}, Figure 4). At t = 0.15 s, these structures detach and are shedded into the wake. These detachments are more amplified in translation configuration than rotation configuration. They occur all along the segment in translation and rather at the level of the hand in rotation. It also appears in

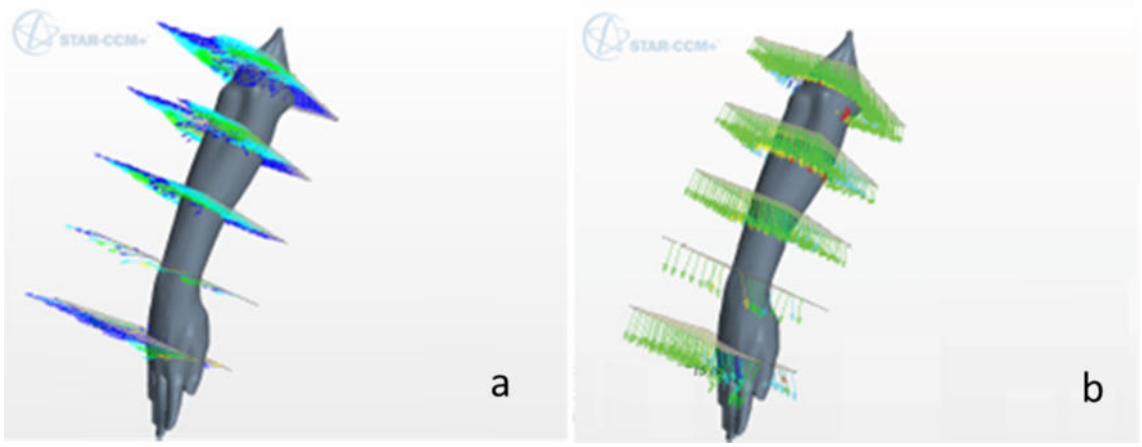

Fig. 2 Visualization of the fluid velocity fields in the hand reference system (X, Y, Z): (a) in translation, (b) in rotation, at t = 0.4 s.

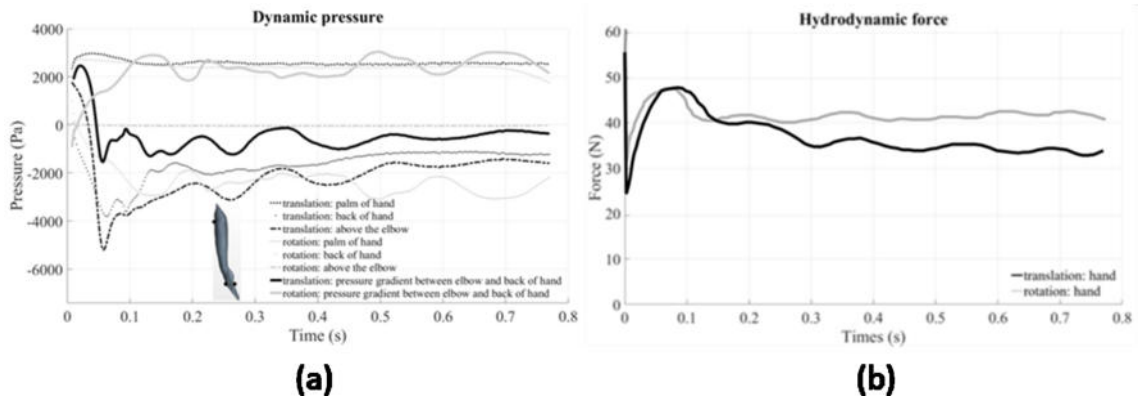

Fig. 3 Comparison of the dynamic pressure (a) and the hydrodynamic forces (b) to the surface of the hand, between the translational (black curves) and rotational (grey curves) configurations.

translation a tip vortex (TV^{trans}) at the fingertip, and a tip vortex in rotation (TV^{rot}, at t = 0.25 s). From t = 0.25 s, two new structures begin to appear in each configuration: TEV_2^{trans}, LEV_2^{trans} and TEV_2^{rot}, LEV_2^{rot}. These structures evolve in translation in rings structure from the elbow to the hand (The TV merge with the TEV, notably in rotation). In translation, the formation at the elbow is essentially due to a tip body, which in reality does not exist since there is normally a joint at the elbow. In both configurations, due to an accumulation of vorticity, a complex entanglement of vortex structures appears on the dorsal side of the hand. From t = 0.35 s in the rotating configuration, there is the presence of more vortices on the dorsal side of the hand relative to the translation configuration. This can be explained by both the effect of the axial flow which translates the vorticity towards the fingertip, and at the same time the effect of the tip vortex at the fingertip which prevents the evacuation of this vorticity.

Thus, in rotation configuration, the vorticity tends to build up on the dorsal side of the hand, and saturate to finally lead to a "bursting" phenomenon (Jardin and David 2015). In contrast, in the translation configuration, there is no axial flow: the vorticity is more easily evacuated throughout the forearm with less accumulation at the hand. According Ramasamy et al. (2005) for high Reynolds numbers (as is the case in swimming, Samson et al., 2015b), the preponderance of inertial forces relative to viscous forces probably affects the balance between the formation rate of the LEV and the axial flow so that the stability of the flow is not ensured. The high Reynolds number then would explain this "burst" phenomenon of vortex structures identified on the dorsal side of the hand. This accumulation of vorticity on the back of the hand would be one of the main causes of the pressure gradient along the direction of the arm.

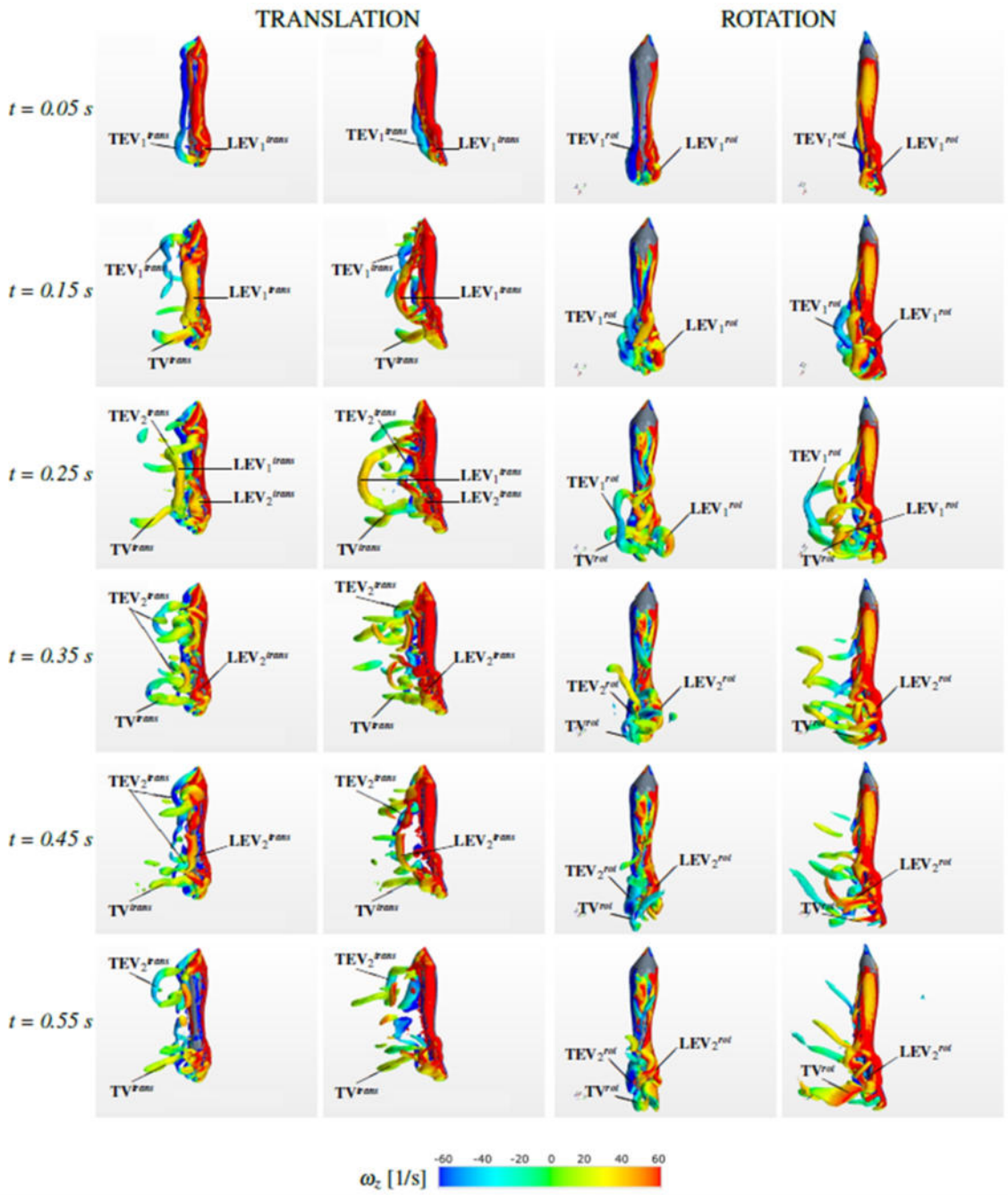

Fig. 4 Comparisons of vortices, in translation (left pictures) and rotation (right pictures) configurations, on the hand and forearm, from t = 0.05 s to t = 0.55 s.

5. Conclusion

The rotation of the arm is thus a movement favorable to the generation of hydrodynamic forces: the vorticity, translated by the axial flow along the forearm accumulates on the back of the hand and creates a pressure gradient from elbow towards the fingertip. This rotational movement is particularly present in the first part of the aquatic path between the end of the stretch phase and the beginning of the insweep. This rotation creates an axial flow which must play an important role in the propulsion. This rotational movement around the elbow is therefore to be taught very early with young swim-

mers, and in particular by an elongation of the arm and a positioning of the elbow placed high as early as possible in the beginning of the aquatic stroke.

Acknowledgement

The authors would like to acknowledge CPER and FEDER for the means of computing mesocenter.

References

Bixler, B., Riewald, S., 2002. Analysis of a swimmer's hand and arm in steady flow conditions using computational fluid dynamics. Journal of Biomechanics 35, 713-717.

Ellington, C. P., Van Den Berg, C., Willmott, A. P., Thomas, A. L., 1996. Leading-edge vortices in insect fl ight. Nature 384, 626-630.

Jardin T., David L., 2014. Spanwise gradients in flow speed help stabilize leading-edge vortices on revolving wings. Physical Review E Vol 90, Issue 1, 013011

Jardin, T., David, L., 2015. Coriolis effects enhance lift on revolving wings. Physical Review E : Statistical, Nonlinear, and Soft Matter Physics, American Physical Society, 91, 1-4.

Kudo, S., Vennell, R., Wilson, B., 2013. The effect of unsteady flow due to acceleration on hydrodynamic forces acting on the hand in swimming. Journal of Biomechanics 46 (10), 1697-1704.

Maglischo, E.W., 2003. Swimming Fastest. Human Kinetics, Champaign, IL.

Matsuuchi, K., Miwa, T., Nomura, T., Sakakibara, J., Shintani, H., Ungerechts, B.E., 2009. Unsteady flow field around a human hand and propulsive force in swimming. Journal of Biomechanics 42, 42-47.

Monnet, T., Samson, M., Bernard, A., David, L., Lacouture, P., 2014. Measurement of three dimensional hand kinematics during swimming with a motion capture system: a feasibility study. Sports Engineering, 17, 171-181.

Ramasamy, M., Leishman, J.G., Singh, B., 2005. Wake structure diagnostics of a flapping wing mav. SAE transactions, 114(1): 907 – 919.

Samson, M., Monnet, T., Bernard, A., Lacouture, P., David, L., 2015a. The role of the entry-and-stretch phase at the different paces of race in front crawl swimming. Journal of Sports Sciences 33(15), 1535-1543.

Samson, M., Monnet, T., Bernard, A., Lacouture, P., David, L., 2015b. Kinematic hand parameters in front crawl at different paces of swimming. Journal of Biomechanics 48, 3743-3750.

Samson, M., Monnet, T., Bernard, A., Lacouture, P., David, L., 2017. Unsteady computational fluid dynamics in front crawl swimming. Computer methods in biomechanics and biomedical engineering 20 (7), 783-793.

Takagi, H., Sanders, R., 2002. Measurement of propulsion by the hand during competitive swimming. In The Engineering of Sport 4 (Eds. Ujihashi, S and Haake, SJ), 631-637, Blackwell Publishing.

Takagi, H., Nakashima, M., Ozaki, T., Matsuuchi, K., 2014. Unsteady hydrodynamic forces acting on a robotic arm and its flow field: Application to the crawl stroke. Journal of Biomechanics 47 (6), 1401-1408.

Takagi, H., Nakashima, M., Sato, Y., Matsuuchi, K., Sanders, R.H., 2016. Numerical and experimental investigations of human swimming motions. Journal of Sports Sciences 34(16), 1564-1580.

Tsunokawa, T., Tsuno, T., Mankyu, H., Takagi, H., Ogita, F., 2018. The effect of paddles on pressure and force generation at the hand during front crawl. Human Movement Science 57, 409-416.

Toussaint, H.M., Van Den Berg, C., Beek, W.J., 2002. Pumped-up propulsion during front crawl swimming. Medicine and Science in Sports and Exercise 34, 314-319.

Von Ellenrieder, K.D., Parker, K., Soria, J., 2003. Flow structures behind a heaving and pitching finite-span wing. Journal of Fluid Mechanics 490, 129-138.